Journal of Applied Analysis and Computation
Volume 14, Number 6, December 2024, 3078–3098
Website:http://www.jaac-online.com
DOI:10.11948/20230453

ANALYSIS OF NOVEL FRACTIONAL ORDER PLASTIC WASTE MODEL AND ITS EFFECTS ON AIR POLLUTION WITH TREATMENT MECHANISM

Hardik Joshi[1], Mehmet Yavuz[2,3,†] and Necati Özdemir[4]

Abstract In the present era, the plastic waste problem is a global challenge due to its massive production. The post-use of waste plastic influences the earth's environment, human life, marine life, and ocean. Thus there is a necessity to develop good strategies for the exclusion of plastic waste. Because of this, an extension is paid on the procedure of burning and recycling plastic waste. As a case study, the four-dimensional systems of ordinary differential equations are developed to estimate the effects of burned plastic and recycled plastic on air pollution. The well-posedness and qualitative properties are discussed. The reproduction number of the plastic waste model and local and global stability are discussed in detail. The effect of influence parameters is systematically investigated by numerical experiments. The numerical results provide a better strategy to restrict air pollution and ensure a good climate, earth's environment, and healthy human life.

Keywords Plastic, burned plastic, recycled plastic, air pollution, fractional order, stability analysis.

MSC(2010) 34A08, 34A34, 34D20, 39A30, 91B76.

1. Introduction

Plastic is a material made from synthetic or semi-synthetic materials and was accidentally found by the German chemist Christian Schonbein. Christian has experimented with a mixture of nitric acid and sulphuric acid on cotton cloth. The chemical reaction occurred and then he placed it over the stove after some time the fabric vanished and became plastic. Plastics do not corrode by water and air whereas almost all metals corrode with them. Due to this reason, it was widely adopted by the field of chemistry and material science as a utensil or storage of chemicals. According to the Society of the Plastics Industry, to recognize plastic by

[†]The corresponding author.
[1]Department of Mathematics, LJ Institute of Engineering and Technology, LJ University, Ahmedabad-382210, Gujarat, India
[2]Department of Mathematics and Computer Sciences, Necmettin Erbakan University, 42090 Konya, Türkiye
[3]Centre for Environmental Mathematics, Faculty of Environment, Science and Economy, University of Exeter, TR10 9FE, United Kingdom
[4]Department of Mathematics, Balıkesir University, 10145 Balıkesir, Türkiye
Email: hardik.joshi8185@gmail.com(H. Joshi), M.Yavuz@exeter.ac.uk(M. Yavuz), nozdemir@balikesir.edu.tr(N. Özdemir)

its classification they introduced a resin identification code. This code categorized the plastic into seven different categories namely polyethylene terephthalate, high-density polyethylene, polyvinyl chloride, low-density polyethylene, polypropylene, polystyrene, and other plastics.

Nowadays, plastics are growingly used in our day-to-day life such as in packaging, consumer products, and transportation as it is easily available and inexpensive. The single usage of plastic bags, food wrappers, beverage bottles, straws, containers, and caps are the various sources and pathways through which plastic waste enters the environment. Also, illegal dumping is the major source of plastic waste detected. In 2020, approximately 400 million tonnes of plastic were produced. According to one estimate, there is only 9 percent of plastic is recycled in total plastic production. Hence plastic pollution becomes a global challenge as it directly influences the earth's environment, human life, marine life, and ocean. Thus to protect the environment we must carefully think about the reduction of plastic waste by applying control measures such as burning plastic, recycled plastic, and as much as reducing the usage of plastic.

Plastic burning is one of the foremost reasons to quickly reduce plastic waste simultaneously diminish the volume of landfills, generate energy, and utilize it for other purposes, limit deforestation, burning heat decompose plastic polymers into minor hydrocarbons that are refined to produce diesel fuel. On the other side, the burning process damages the environment and the quality of air. It releases various toxic gases, hydrochloric acid, dioxins, and sulfur dioxide and significantly invites many diseases like asthma, pneumonia, skin irritations, liver, kidney, and cancer. Thus it is essential to manage or mitigate the health risks associated with burning plastic waste. Identify the plastic types that generate more toxicity during burning then use a gasification process. Promote the repalletization and remolding of plastic waste instead of burning them. Encourage the usage of water during the burning process that significantly dissolves the hazardous gases. Burning of inorganic plastic waste in the open with unrestrained fire is unsafe. Also follows the guidelines given by the central pollution control board and state authority and burns only approved plastics. The recycling of plastic is also the procedure to reduce plastic waste and transfer it into usable products. Recycling plastic waste reduces the need to produce new raw materials, emissions of carbon dioxide and hazardous gases into the air, spread rubbish to landfills, and plastic waste. This procedure significantly improved the air quality and environment as it protected from the emission of dangerous gases. Simultaneously, the recycling process diminishes the requirement for the production of plastic and saves energy.

Air pollution mainly occurs due to the defilement of air level as the scant stuff is mixing with it. It disturbs the natural environment and the quality of air and when it goes to breathing then it damages the living organism and as results invite several diseases. This situation is happened for a longer period then it leads to the death of persons. According to the World Health Organization, 99 percent population of the world is living where the quality of air level is not adequate [47]. Due to this reason, in 2019 an estimated 4.2 million in the globe are met to the premature deaths [47].

To resolve or overcome this situation few theoretical attempts are registered in the form of a mathematical model. The mathematical model is a great tool to overcome any worst situation in the absence of experimental work. Nowadays mathematical models are gaining more attention due to the development of computer technology and their applicability in almost all areas of science, technology, earth science, biology, neuroscience, medicine, and so on [1, 2, 5, 9, 14–17, 20–27, 29, 33–36, 38, 39, 41–44]. Chaturvedi et al. have developed a mathematical model to study the effect of plastic waste on the surface of the ocean [6]. Barma et al. have developed a mathematical model for municipal solid waste and examine the establishment of recycling, composting, and combusting centers for optimum cost [4]. Izadi et al. have developed a waste plastic model to examine the effects of marine debris and recycling on the ocean environment [19]. Besides this mathematical approach, various attempts have been made to study the cause and optimal solution of plastic waste on air pollution and the environment with different statistical techniques and case studies [7, 8, 10, 18, 28, 46, 48]. Thus it is observed from the literature that seldom mathematical attempts are registered to manage plastic waste and its side effects on the environment. Thus motivated by this, in this study we have developed a mathematical plastic waste model to study the impact of burned plastic and recycled plastic on air pollution. To the best of the author's knowledge to date, none of the mathematical models has provided a deep insight into the control of plastic waste and air pollution.

The paper is organized as follows. In Section 2, we provide the basic definition of the fractional derivative. In Section 3, we introduce the novel plastic waste model and then extend it to fractional order. In Section 4, we discuss its various equilibria and local and global stability behavior. In Section 5, numerical experiments are performed to validate the analytical findings and develop a treatment mechanism to control air pollution. Finally, we conclude some important results in Section 6.

2. Preliminaries of plastic waste model

Some basic definitions of fractional derivatives and their Laplace transform are recalled in this section which is important for this study [3, 12, 31, 37, 40].

Definition 2.1. Let $f(t)$ be a function $f : \mathbb{R}^+ \to \mathbb{R}$ then the Riemann-Liouville fractional integral is defined as

$$ {}^{RL}I^{\alpha}_{0+}f(t) = \frac{1}{\Gamma(\alpha)} \int_0^t (t-w)^{\alpha-1} f(w)dw, \tag{2.1}$$

where α is the order of derivatives and $t > 0$.

Definition 2.2. Let $f(t)$ be a function $f : \mathbb{R}^+ \to \mathbb{R}$ then the Riemann-Liouville fractional derivative is defined as

$$ {}^{RL}D^{\alpha}_{0+}f(t) = D^n \, {}^{RL}I^{n-\alpha}_{0+} f(t), \tag{2.2}$$

where α is the order of derivative, D is the classical derivative and $t > 0$.

Definition 2.3. The Caputo fractional derivative (CFD) of a function $f(t)$ is defined as

$$ {}^{C}D^{\alpha}_{0+}f(t) = {}^{RL}I^{n-\alpha}_{0+} D^n f(t) = \frac{1}{\Gamma(n-\alpha)} \int_0^t (t-w)^{n-\alpha-1} f^n(w)dw, \tag{2.3}$$

where $\alpha \in (n-1, n)$ is the order of derivatives and $n \in \mathbb{N}$.

Definition 2.4. The Laplace transform of CFD of a function $f(t)$ is given by

$$L\{^C D_{0+}^{\alpha} f(t)\} = s^{\alpha} F(s) - \sum_{j=0}^{n-1} s^{\alpha-j-1} f^{(j)}(0). \tag{2.4}$$

3. Mathematical model

In this section, we have developed a mathematical model for plastic waste and analyzed it to examine the impact on air pollution. The burning and recycling of plastic, two strategies are adopted in the model for the reduction of plastic waste. The model is divided into four compartments plastic $P(t)$, burned plastic $B(t)$, recycled plastic $R(t)$, and air pollution $A(t)$. The constant demand rate of plastic Λ is considered, β represents the burning rate of plastic, δ represents the rate of air pollution through burned plastic, θ represents the recycling rate of plastic, ρ represents the rate of recycling plastic for reused, φ represents the burning rate of recycled plastic for high temperature, γ represents the rate of air pollution through recycling plastic, ω represents the rate of disposable plastic or recovery rate from each compartment. A schematic diagram in Figure 1 represents this situation.

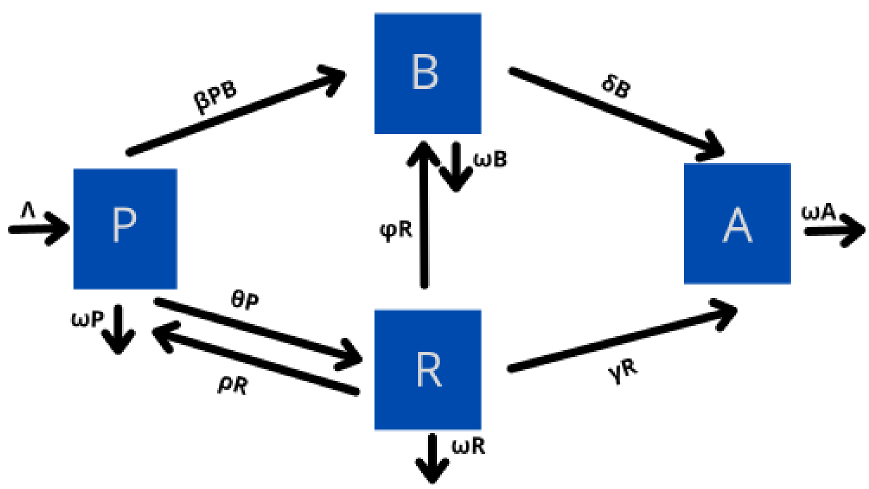

Figure 1. Flow diagram of the PBRA model.

Thus by considering this situation the set of nonlinear ordinary differential equations for the plastic waste model is described as follows

$$\begin{aligned}
\frac{dP}{dt} &= \Lambda - \beta PB - \theta PR + \rho R - \omega P,\\
\frac{dB}{dt} &= \beta PB + \varphi R - \delta B - \omega B,\\
\frac{dR}{dt} &= \theta PR - \rho R - \varphi R - \gamma R - \omega R,\\
\frac{dA}{dt} &= \delta B + \gamma R - \omega A,
\end{aligned} \tag{3.1}$$

Table 1. Description of the model parameters.

Parameter	Description of parameter
Λ	Demand rate
β	Burning rate
θ	Recycling rate
ρ	Recycle or reused rate
ω	Wastage rate
φ	Burning rate through recycling process
δ	Air pollution rate due to burned plastic
γ	Air pollution rate due to the recycling process of plastic

along with the initial conditions $P(0) = P_0, B(0) = B_0, R(0) = R_0$, and $A(0) = A_0$. The plastic waste model parameters and their description are listed in Table 1.

Here, we consider the fractional derivative approach to involve the impact of vertical transmission in the plastic waste model. The term vertical transmission stands for the transfer of plastic from one generation to the next generation through recycling or reproduction which is the process of heredity. Fractional derivatives are non-local operators and can best describe heredity phenomena in the dynamical system. Also, the fractional order model best describes the heredity traits, anomalous diffusion, and mechanical properties of materials whereas the integer order model fails. A fractional differential equation is a generalization of an ordinary differentiation equation as it provides a great degree of freedom to choose the order of derivative [3, 12, 31, 37, 40]. It can be applied in the linear as well as nonlinear differential equation in a straightforward manner as an ordinary differentiation equation. This model (3.1) is transformed in the form of fractional differential equations as follows

$$\begin{aligned}
{}_0^C D_t^\alpha P &= \Lambda - \beta PB - \theta PR + \rho R - \omega P, \\
{}_0^C D_t^\alpha B &= \beta PB + \varphi R - \delta B - \omega B, \\
{}_0^C D_t^\alpha R &= \theta PR - \rho R - \varphi R - \gamma R - \omega R, \\
{}_0^C D_t^\alpha A &= \delta B + \gamma R - \omega A,
\end{aligned} \tag{3.2}$$

with the initial conditions $P(0) = P_0, B(0) = B_0, R(0) = R_0$, and $A(0) = A_0$. Note that when the order of the derivative is reached $\alpha = 1$ then the fractional PBRA model (3.2) converts to the original PBRA model (3.1).

4. Model analysis

In this section, the positivity and boundedness of the proposed PBRA model (3.2) are derived.

4.1. Positivity and boundedness

Lemma 4.1. [37] *Let $f(t)$ be a continuous function on $[a,b]$ and the CFD of $f(t)$ is also a continuous function for $0<\alpha\le 1$ then for every $t\in(a,b]$ we have*

$$f(t)=f(a)+\frac{1}{\Gamma(\alpha)}{}_0^C D_t^\alpha f(\tau)(t-a)^\alpha, \tag{4.1}$$

where $0\le\tau\le t$.

If $f(t)$ be a continuous function on $[a,b]$ and for every $t\in(0,b]$ we have ${}_0^C D_t^\alpha f(t)\ge 0$, for $0<\alpha\le 1$ then $f(t)$ is positive for all t.

Theorem 4.1. *If the initial conditions of the PBRA model (3.2) are in the region Ω and it is defined as $\Omega=\left\{(P,B,R,A)\in\mathbb{R}_+^4 \,\middle|\, P,B,R,A\ge 0\right\}$ than all the possible solutions of the model are lying within in Ω.*

Proof. Let's consider the first equation of the model (3.2)

$${}_0^C D_t^\alpha P|_{P=0}=\Lambda+\rho R\ge 0, \tag{4.2}$$

as Λ the demand rate of plastic and ρ the recycling rate of plastic are positive parameters.

Similarly, we have

$$\begin{aligned}
&{}_0^C D_t^\alpha B|_{B=0}=\varphi R\ge 0,\\
&{}_0^C D_t^\alpha R|_{R=0}=0,\\
&{}_0^C D_t^\alpha A|_{A=0}=\delta B+\gamma R\ge 0.
\end{aligned} \tag{4.3}$$

Equations (4.2)-(4.3) hold for all the points in the region, hence, by using Lemma 4.1 we confirmed that the given region is positive invariant. Next, we prove the boundedness of the proposed PBRA model.

To obtain the total demand for plastic we add the equations of the model (3.2) then we get

$${}_0^C D_t^\alpha T(t)=\Lambda-\omega P-\omega B-\omega R-\omega A, \tag{4.4}$$

where $T(t)=P(t)+B(t)+R(t)+A(t)$.

Thus we have

$${}_0^C D_t^\alpha T(t)=\Lambda-\omega T. \tag{4.5}$$

Hence to confirm the boundedness of the model we solve the following fractional initial value problem

$${}_0^C D_t^\alpha T(t)+\omega T=\Lambda, \tag{4.6}$$

with $T(0)=T_0$.

By applying the Laplace transform to both sides of the equation (4.6) we have

$$L\left({}_0^C D_t^\alpha T(t)+\omega T\right)=L(\Lambda). \tag{4.7}$$

Then by using equation (2.4) equation (4.7) is transformed as

$$\bar{T}(s)=\frac{s^{-1}\Lambda}{s^\alpha+\omega}+\frac{s^{\alpha-1}T_0}{s^\alpha+\omega}. \tag{4.8}$$

Next by inverting the Laplace transform of equation (4.8), we have

$$T(t)=\Lambda t^\alpha E_{\alpha,\alpha+1}(-\omega t^\alpha)+E_{\alpha,1}(-\omega t^\alpha)T_0$$

$$
\begin{aligned}
&\leq \frac{\Lambda}{\omega}\left(t^{\alpha}\omega E_{\alpha,\alpha+1}(-\omega t^{\alpha})\right) + E_{\alpha,1}(-\omega t^{\alpha})\\
&\leq \frac{\Lambda}{\omega}\frac{1}{\Gamma(1)}\\
&\leq \frac{\Lambda}{\omega}. \qquad (4.9)
\end{aligned}
$$

Hence, equation (4.9) confirmed the boundedness of the model (3.2). □

Theorem 4.2. *The PBRA model (3.2) possesses three equilibrium points namely (I) Pollution free equilibrium (PFE) point E^P (II) Recycling free equilibrium (RFE) point E^R (III) Endemic equilibrium point (EEP) E^*.*

Proof. To determine the equilibrium point of the model (3.2), we simultaneously solve the following equations

$$
{}_0^C D_t^{\alpha} P(t) = {}_0^C D_t^{\alpha} B(t) = {}_0^C D_t^{\alpha} R(t) = {}_0^C D_t^{\alpha} A(t) = 0. \qquad (4.10)
$$

Then we reach the set of algebraic equations as

$$
\begin{aligned}
&\Lambda - \beta PB - \theta PR + \rho R - \omega P = 0,\\
&\beta PB + \varphi R - \delta B - \omega B = 0,\\
&\theta PR - \rho R - \varphi R - \gamma R - \omega R = 0,\\
&\delta B + \gamma R - \omega A = 0.
\end{aligned} \qquad (4.11)
$$

Then the simple algebraic calculation provides the three solutions to equation (4.11). The first solution is known as the PFE point $E^P = (P^P, B^P, R^P, A^P)$, where

$$
P^P = \frac{\Lambda}{\omega}, B^P = R^P = A^P = 0. \qquad (4.12)
$$

The second solution is known as the RFE point $E^R = (P^R, B^R, R^R, A^R)$, where

$$
P^R = \frac{\delta - \omega}{\beta}, B^R = \frac{\Lambda\beta - \omega(\delta+\omega)}{\beta(\delta+\omega)}, R^R = 0, A^R = \frac{\delta(\Lambda\beta - \omega(\delta+\omega))}{\beta\omega(\delta+\omega)}, \qquad (4.13)
$$

and the third solution is known as EEP $E^* = (P^*, B^*, R^*, A^*)$, where

$$
\begin{aligned}
P^* &= \frac{\rho+\gamma+\varphi+\omega}{\theta}, B^* = \frac{\varphi(\omega(\rho+\gamma+\varphi+\omega) - \Lambda\theta)}{((\rho+\gamma+\varphi+\omega)(\beta(\gamma+\omega) - \theta(\delta+\omega)) + \theta\rho(\delta+\omega))},\\
R^* &= \frac{(\omega(\rho+\gamma+\varphi+\omega) - \Lambda\theta)(\theta(\delta+\omega) - \beta(\rho+\gamma+\varphi+\omega))}{\theta(((\rho+\gamma+\varphi+\omega)(-\theta(\delta+\omega) + \beta(\gamma+\omega))) + \theta\rho(\delta+\omega))},\\
A^* &= \frac{(\omega(\rho+\gamma+\varphi+\omega) - \Lambda\theta)(\theta(\gamma(\delta+\omega) + \delta\varphi) - \beta(\rho+\gamma+\varphi+\omega))}{\theta\omega(((\rho+\gamma+\varphi+\omega)(-\theta(\delta+\omega) + \beta(\gamma+\omega))) + \theta\rho(\delta+\omega))}.
\end{aligned} \qquad (4.14)
$$

This completes the proof. □

4.2. Basic reproduction number

The basic reproduction number (R_0) in epidemiology shows the transmissibility of infectious pathogens. Here R_0 shows how pollution spreads through the pollutant class that is the burning and recycling process of plastic. That provides information about influence parameters and supports to development of an efficient public health policy to control or restrict air pollution. The basic reproduction number of the PBRA model is obtained by using the next-generation matrix method [11]. For that, we have considered the right-hand side of the pollutant class B and R and rearranged in the following system as

$$ {}_0^C D_t^\alpha x = F(x) - V(x), \tag{4.15} $$

where $x = [B, R]^T$, F is the term containing the pollution rate, and V containing the other terms.

The Jacobian matrices of $F(x)$ and $V(x)$ at the PFE point E^P are

$$ F(x) = \begin{pmatrix} \Lambda\beta/\omega & 0 \\ 0 & 0 \end{pmatrix}, V(x) = \begin{pmatrix} \delta+\omega & -\varphi \\ 0 & \rho+\gamma+\varphi+\omega-\Lambda\theta/\omega \end{pmatrix}. \tag{4.16} $$

Now,

$$ \begin{aligned} FV^{-1} &= \begin{pmatrix} \Lambda\beta/\omega & 0 \\ 0 & 0 \end{pmatrix} \begin{pmatrix} 1/(\delta+\omega) & \varphi/((\delta+\omega)(\rho+\gamma+\varphi+\omega-\Lambda\theta/\omega)) \\ 0 & 1/(\rho+\gamma+\varphi+\omega-\Lambda\theta/\omega) \end{pmatrix} \\ &= \begin{pmatrix} \frac{\Lambda\beta}{\omega(\delta+\omega)} & \frac{\beta P\varphi}{(\delta+\omega)(\rho+\gamma+\varphi+\omega-\Lambda\theta/\omega)} \\ 0 & 0 \end{pmatrix}. \end{aligned} \tag{4.17} $$

The spectral radius of FV^{-1} known as the basic reproduction number and is defined by R_0 as

$$ R_0 = \frac{\Lambda\beta}{\omega(\delta+\omega)}. \tag{4.18} $$

Theorem 4.3. *The PFE point $E^P = (P^P, B^P, R^P, A^P)$ of the model (3.2) is locally asymptotically stable if $R_0 < 1$ and under the condition*

$$ \frac{\Lambda\theta}{\omega} < (\rho+\gamma+\varphi+\omega), \tag{4.19} $$

otherwise unstable.

Proof. The Jacobian matrix for the model (3.2) is given by

$$ J = \begin{bmatrix} -(\beta B+\theta R+\omega) & -\beta P & \rho-\theta P & 0 \\ \beta B & \beta P-(\delta+\omega) & \varphi & 0 \\ \theta R & 0 & \theta P-(\rho+\varphi+\gamma+\omega) & 0 \\ 0 & \delta & \gamma & -\omega \end{bmatrix}. \tag{4.20} $$

The Jacobian matrix at the PFE point E^P is

$$ J(E^P) = \begin{bmatrix} -\omega & -\Lambda\beta/\omega & \rho-\Lambda\theta/\omega & 0 \\ 0 & \Lambda\beta/\omega-(\delta+\omega) & \varphi & 0 \\ 0 & 0 & \Lambda\theta/\omega-(\rho+\varphi+\gamma+\omega) & 0 \\ 0 & \delta & \gamma & -\omega \end{bmatrix}. \tag{4.21} $$

The Jacobian matrix $J(E^P)$ possesses four Eigenvalues $\lambda_1, \lambda_2, \lambda_3$ and λ_4 as follows

$$\lambda_1 = \lambda_2 = -\omega, \lambda_3 = \frac{\Lambda\theta - \omega(\rho + \varphi + \gamma + \omega)}{\omega}, \lambda_4 = \frac{\Lambda\beta - \omega(\delta + \omega)}{\omega}. \tag{4.22}$$

The first and second Eigenvalues are negative. To determine the nature of the fourth Eigen value we rearranged as follows

$$\lambda_4 = \frac{\Lambda\beta - \omega(\delta + \omega)}{\omega} = (\delta + \omega)\left(\frac{\Lambda\beta}{\omega(\delta + \omega)} - 1\right) = (\delta + \omega)(R_0 - 1). \tag{4.23}$$

Hence $\lambda_4 < 0$ if $R_0 < 1$. The third Eigenvalues $\lambda_3 < 0$ if

$$\frac{\Lambda\theta - \omega(\rho + \varphi + \gamma + \omega)}{\omega} < 0. \tag{4.24}$$

Therefore to confirm the PFE point E^P is locally asymptotically stable it must satisfy the condition $\frac{\Lambda\theta}{\omega} < (\rho + \gamma + \varphi + \omega)$. This completes the proof. □

Theorem 4.4. *The RFE point* $E^R = (P^R, B^R, R^R, A^R)$, *of the model (3.2) is locally asymptotically stable if* $R_0 < 1$ *and under the condition*

$$\frac{\theta(\delta + \omega)}{\beta} < (\rho + \varphi + \gamma + \omega), \tag{4.25}$$

otherwise unstable.

Proof. We calculate the Jacobian matrix given in equation (4.20) at the RFE point E^R as follows

$$J(E^R) = \begin{bmatrix} -\dfrac{\Lambda\beta}{(\delta + \omega)} & -(\delta + \omega) & \rho\beta - \theta(\delta + \omega) & 0 \\ \dfrac{\Lambda\beta - \omega(\delta + \omega)}{(\delta + \omega)} & 0 & \varphi & 0 \\ 0 & 0 & \dfrac{\theta(\delta + \omega)}{\beta} - (\rho + \varphi + \gamma + \omega) & 0 \\ 0 & \delta & \gamma & -\omega \end{bmatrix}. \tag{4.26}$$

The Jacobian matrix $J(E^R)$ possesses four Eigenvalues $\lambda_1, \lambda_2, \lambda_3$ and λ_4 as follows

$$\begin{aligned} \lambda_1 = -\omega, \lambda_2 &= \frac{\theta(\delta + \omega) - \beta(\rho + \varphi + \gamma + \omega)}{\beta}, \\ \lambda_{3,4} &= \frac{-\Lambda\beta \pm \sqrt{\Lambda^2\beta^2 + 4\omega(\delta + \omega)^3 - 4\Lambda\beta(\delta + \omega)^2}}{2(\delta + \omega)}. \end{aligned} \tag{4.27}$$

The first Eigenvalue is negative. The second Eigenvalue $\lambda_2 < 0$ if

$$\frac{\theta(\delta + \omega) - \beta(\rho + \varphi + \gamma + \omega)}{\beta} < 0. \tag{4.28}$$

Therefore to confirm $\lambda_2 < 0$ it must satisfy the condition $\frac{\theta(\delta+\omega)}{\beta} < (\rho + \varphi + \gamma + \omega)$. To determine the nature of the remaining two Eigen value we rearranged them as follows

$$\lambda_{3,4} = \frac{-\Lambda\beta \pm \sqrt{\Lambda^2\beta^2 + 4\omega(\delta + \omega)^2 \left\{\omega(\delta + \omega)(1 - R_0)\right\}}}{2(\delta + \omega)}. \tag{4.29}$$

Therefore to confirm the RFE point E^R is locally asymptotically stable it must satisfy $R_0 < 1$ along with the condition (4.25). This completes the proof. □

Theorem 4.5. *The EEP point $E^* = (P^*, B^*, R^*, A^*)$, of the model (3.2) is locally asymptotically stable if $R_0 < 1$ and under the condition*

$$\beta(\rho+\gamma+\varphi+\omega) < \frac{\theta(\delta+\omega)}{\beta}, \tag{4.30}$$

otherwise unstable.

Proof. The Jacobian matrix for the model (3.2) is given by

$$J = \begin{bmatrix} -(\beta B+\theta R+\omega) & -\beta P & \rho-\theta P & 0 \\ \beta B & \beta P-(\delta+\omega) & \varphi & 0 \\ \theta R & 0 & \theta P-(\rho+\varphi+\gamma+\omega) & 0 \\ 0 & \delta & \gamma & -\omega \end{bmatrix}. \tag{4.31}$$

The Jacobian matrix at the EEP E^* is

$$J(E^*) = \begin{bmatrix} -(\beta B^*+\theta R^*+\omega) & -\beta P^* & \rho-\theta P^* & 0 \\ \beta B^* & \beta P^*-(\delta+\omega) & \varphi & 0 \\ \theta R^* & 0 & \theta P^*-(\rho+\varphi+\gamma+\omega) & 0 \\ 0 & \delta & \gamma & -\omega \end{bmatrix}. \tag{4.32}$$

The characteristic polynomial for the Jacobian matrix $J(E^*)$ is

$$\lambda^4 + a_1\lambda^3 + a_2\lambda^2 + a_3\lambda + a_4 = 0, \tag{4.33}$$

where

$$\begin{aligned} a_1 &= (\beta B^*+\theta R^*+\omega)+\omega+k_1+k_2, \\ a_2 &= (\beta^2 B^* P^* + P^* R^* \theta^2 + R^*\theta\rho) + k_1(\beta B^*+\theta R^*+\omega) + k_2(\beta B^*+\theta R^*+\omega) \\ &\quad + \omega(\beta B^*+\theta R^*+\omega) + (k_1k_2+\omega k_1+\omega k_2), \\ a_3 &= (\beta^2 B^* P^* k_2 + \omega\beta^2 B^* P^* + \beta P^* R^*\theta\varphi + P^* R^*\theta^2 k_1 + \omega P^* R^* \theta^2 + R^*\theta\rho k_1 \\ &\quad + \omega k_1 k_2 + \omega R^*\theta\rho + k_1k_2(\beta B^*+\theta R^*+\omega) \\ &\quad + \omega k_1(\beta B^*+\theta R^*+\omega) + \omega k_2(\beta B^*+\theta R^*+\omega)), \\ a_4 &= \omega(\beta^2 B^* P^* k_2 + \beta P^* R^*\theta\varphi + P^* R^*\theta^2 k_1 + R^*\theta\rho k_1 + k_1k_2(\beta B^*+\theta R^*+\omega)), \end{aligned} \tag{4.34}$$

and

$$\begin{aligned} k_1 &= (\delta+\omega)-\beta P^*, \\ k_2 &= (\rho+\varphi+\gamma+\omega)-\theta P^*. \end{aligned} \tag{4.35}$$

The model (3.2) is locally asymptotically stable we must ensure that the roots of the equation (4.33) are negative. Then by the Routh-Hurwitz stability criteria [32], it is necessary and sufficient to show that $a_j > 0, j = 1, 2, 3, 4$.

Thus to meet this criteria it must satisfy $R_0 < 1$ along with $k_1, k_2 > 0$. Hence the EEP E^* of the model (3.2) is locally asymptotically stable if $R_0 < 1$ and under the condition (4.30). This completes the proof. □

Lemma 4.2. [45] *Let $f(t) \in \mathbb{R}^+$ be a differentiable and continuous function on $[0,t]$. Then for any $f^* \in \mathbb{R}^+$ we have*

$$ {}_0^C D_t^\alpha \left[f(t) - f^* - f^* \ln \frac{f(t)}{f^*} \right] \le \left(1 - \frac{f^*}{f(t)}\right) {}_0^C D_t^\alpha f(t), \tag{4.36} $$

where $\alpha \in (0,1)$.

Lemma 4.3. [30] *Let $f(t)$ be a locally Lipschiptz function defined over a domain $S \subset \mathbb{R}^n$ and $\Omega \subset S$ be a compact positively invariant with respect to $y' = f(t)$. Let $L(t)$ be a C^1 function defined over S such that $L'(t) \le 0$ in Ω. Let P be the set of all points in Ω where $L'(t) = 0$, and F be the largest invariant set in P. Then, every solution starting in Ω approaches F as $t \to \infty$, means that $d(y(t,t_0), F) \to 0, \mathrm{as} t \to \infty$, for all $t_0 \in \Omega$.*

Theorem 4.6. *The EEP point $E^* = (P^*, B^*, R^*, A^*)$, of the model (3.2) is globally asymptotically stable if $R_0 > 1$ otherwise unstable.*

Proof. Let's consider the positive definite Lyapunov function $L(P, B, R, A) : \Omega \to \mathbb{R}^+$ defined by

$$ \begin{aligned} L(t) =& W_1 \left[P - P^* - P^* \ln\left(\frac{P}{P^*}\right)\right] + W_2 \left[B - B^* - B^* \ln\left(\frac{B}{B^*}\right)\right] \\ &+ W_3 \left[R - R^* - R^* \ln\left(\frac{R}{R^*}\right)\right], \end{aligned} \tag{4.37} $$

where $W_1 = \frac{1}{\omega}, W_2 = \frac{(R_0-1)}{\delta+\omega}, R_0 > 1$ and $W_3 = \frac{1}{(\rho+\varphi+\gamma+\omega)}$ are positive constants. The CFD of the Lyapunov function is obtained as follows

$$ \begin{aligned} {}_0^C D_t^\alpha L(t) =& \frac{1}{\omega} {}_0^C D_t^\alpha \left[P - P^* - P^* \ln\left(\frac{P}{P^*}\right)\right] \\ &+ \frac{(R_0-1)}{\delta+\omega} {}_0^C D_t^\alpha \left[B - B^* - B^* \ln\left(\frac{B}{B^*}\right)\right] \\ &+ \frac{1}{(\rho+\varphi+\gamma+\omega)} {}_0^C D_t^\alpha \left[R - R^* - R^* \ln\left(\frac{R}{R^*}\right)\right]. \end{aligned} \tag{4.38} $$

Then by applying the results of Lemma 4.2, we have

$$ \begin{aligned} {}_0^C D_t^\alpha L(t) \le& \frac{1}{\omega}\left(1 - \frac{P^*}{P(t)}\right) {}_0^C D_t^\alpha P(t) + \frac{(R_0-1)}{\delta+\omega}\left(1 - \frac{B^*}{B(t)}\right) {}_0^C D_t^\alpha B(t) \\ &+ \frac{1}{(\rho+\varphi+\gamma+\omega)}\left(1 - \frac{R^*}{R(t)}\right) {}_0^C D_t^\alpha R(t). \end{aligned} \tag{4.39} $$

Table 2. The numerical value of the PBRA model.

Parameter	Value	Parameter	Value
Λ	0.05	β	0.35
θ	0.40	ρ	0.2
ω	0.30	φ	0.05
δ	0.40	γ	0.30

From equation (3.2), we get

$$\begin{aligned} {}_0^C D_t^\alpha L(t) \leq & \tfrac{1}{\omega}\left(1-\tfrac{P^*}{P(t)}\right)(\Lambda-\beta PB-\theta PR+\rho R-\omega P) \\ & + \tfrac{(R_0-1)}{\delta+\omega}\left(1-\tfrac{B^*}{B(t)}\right)(\beta PB+\varphi R-\delta B-\omega B) \\ & + \tfrac{1}{(\rho+\varphi+\gamma+\omega)}\left(1-\tfrac{R^*}{R(t)}\right)(\theta PR-\rho R-\varphi R-\gamma R-\omega R). \end{aligned} \tag{4.40}$$

From equation (4.14), we have the following relationship between $E^* = (P^*, B^*, R^*, A^*)$

$$\begin{aligned} & \Lambda-\beta P^*B^*-\theta P^*R^* = \omega P^*-\rho R^*, \\ & \beta P^*B^*+\varphi R^* = (\delta+\omega)B^*, \\ & \theta P^*R^* = (\rho+\varphi+\gamma+\omega)R^*. \end{aligned} \tag{4.41}$$

Then by plugging the values of equation (4.41) into equation (4.40) we have

$${}_0^C D_t^\alpha L(t) \leq -\left\{\frac{(P-P^*)^2}{P}+\frac{(B-B^*)^2}{B}(R_0-1)+\frac{(R-R^*)^2}{R}\right\}. \tag{4.42}$$

Thus it is clear that if $R_0 > 1$ then ${}_0^C D_t^\alpha L(t) \leq 0$, and if $P = P^*, B = B^*$ and $R = R^*$ then we get ${}_0^C D_t^\alpha L(t) = 0$. Hence by LaSalle's extension to Lyapunov's principle provided in Lemma 4.3, the EEP point E^* of the model (3.2) is globally asymptotically stable if $R_0 > 1$. The global asymptotic stability confirmed that any trajectories starting from any initial conditions in the domain finally tend to the EEP point of the system. □

5. Numerical results and discussion

In this section, the numerical simulation of the PBRA model is carried out to analyze the effect of burned plastic and recycled plastic on air pollution. The initial conditions are chosen to be $P(0) = 5, B(0) = 2.5, R(0) = 1.25$ and $A(0) = 2$. The parameter values used for numerical simulation are given in Table 2. Using the Adams-type predictor-corrector numerical method developed by Diethelm et al. [13], the PBRA model is simulated for different values of burning rate, recycling rate, reused rate, air pollution rate due to burned and recycled plastic, and fractional order to analyze the dynamical behavior of the model. The numerical results are performed using MATLAB software and simulated in window core(TM) i5-6500 CPU @ 3.20 GHz Processing speed and 8 GB memory.

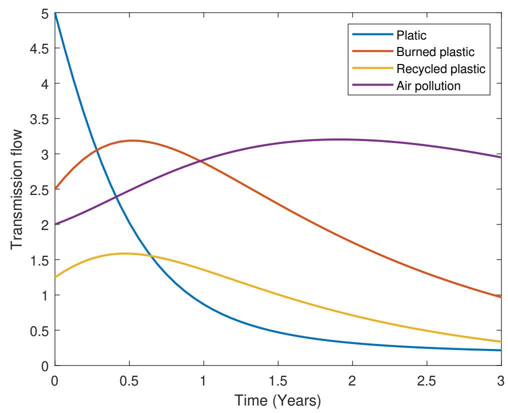

Figure 2. Dynamic behavior of the PBRA model.

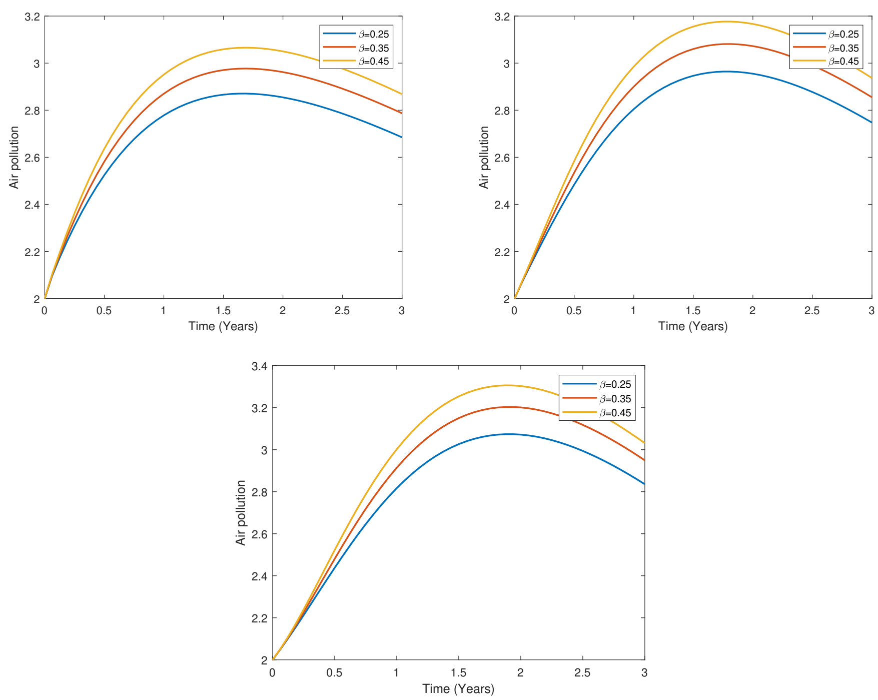

Figure 3. Effect of burning rate on air pollution for (a) $\alpha = 0.8$ (b) $\alpha = 0.9$ (c) $\alpha = 1$.

Figure 2 shows the dynamical behavior of the PBRA model (3.2) which demonstrates the initial state as well as the long-term behavior of the model. Initially, the demand for plastic is high then gradually it decreases as the community uses the plastic from recycled plastic. As time is increased air pollution is leisurely increased due to the burning and recycling process of plastic. The dynamic behavior is calculated for the three years for fractional order $\alpha = 1$ along with the model parameters.

Figure 3-Figure 7 show the impact of burning, recycling, reused, pollution due

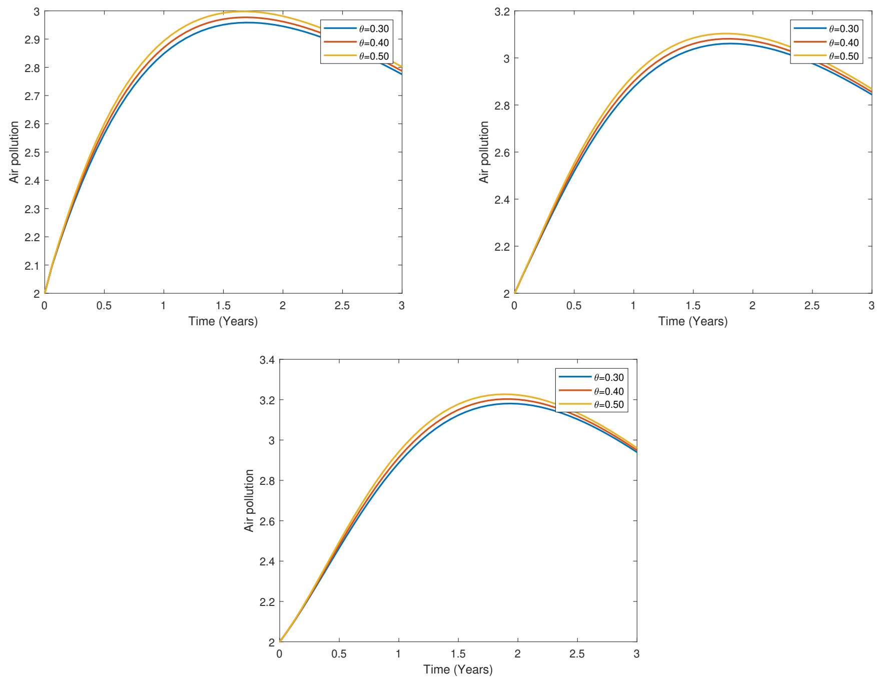

Figure 4. Effect of recycling rate on air pollution for (a) $\alpha = 0.8$ (b) $\alpha = 0.9$ (c) $\alpha = 1$.

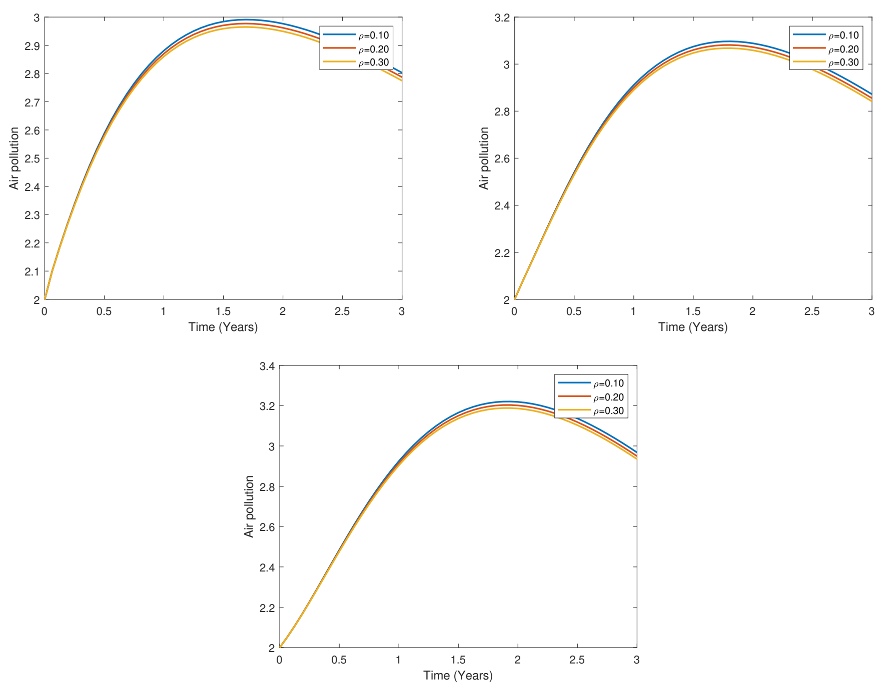

Figure 5. Effect of reused plastic on air pollution for (a) $\alpha = 0.8$ (b) $\alpha = 0.9$ (c) $\alpha = 1$.

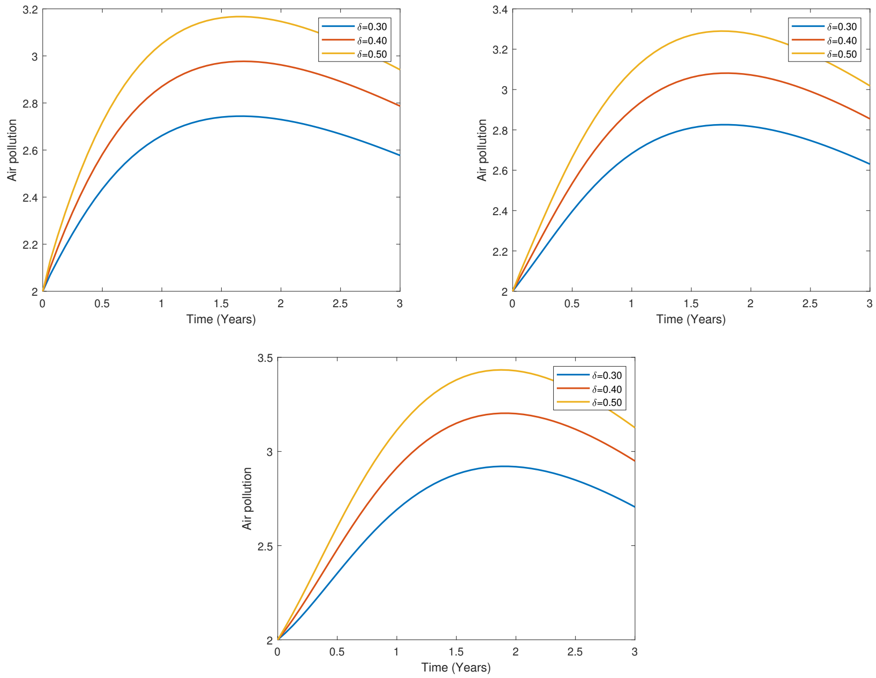

Figure 6. Effect of air pollution due to burned plastic on air pollution for (a) $\alpha = 0.8$ (b) $\alpha = 0.9$ (c) $\alpha = 1$.

to burning, and pollution due to recycling plastic over air pollution. The order of fractional derivatives is considered $\alpha = 0.8, \alpha = 0.9$, and $\alpha = 1$ in subfigures (a) to (c) respectively to capture the effects of vertical transmission. The burning of plastics releases black carbon, organic carbon, polycyclic aromatic hydrocarbons, and greenhouse gases into the air. Figure 3 reveals that as we increase the burning rate from 0.25 to 0.45, large amounts of particles and gases are released into to air that damage the climate and raise air pollution. By simultaneously comparing the results of Figure 3 (a-c), it is observed that for $\alpha = 1$, there is high air pollution compared to $\alpha = 0.8$. This result reveals that vertical transmission also plays a significant role in reducing air pollution. Recycling plastic reduces energy, emission of carbon dioxide, and toxic gases, and ultimately controls air pollution. But when the recycling of plastic waste is executed at a high burning rate then causes air pollution. Figure 4 reveals that a subtle rise in air pollution is observed as we increase the recycling rate from 0.30 to 0.50. By simultaneously comparing the results of Figure 4 (a-c), it is observed that for $\alpha = 1$, there is high air pollution compared to $\alpha = 0.8$. This result reveals that vertical transmission also plays a significant role in reducing air pollution. Also, the graphical results show that as the recycling rate increases air pollution increases but is minimal compared to the burning rate. From Figure 5, it is observed that as the community adopts the reused plastic or its rate increases the air pollution decreases. It is observed that promoting the reuse of plastic and vertical transmission both are crucial strategies for reducing air pollution. From Figure 6, it is observed that as the plastic is burned at a high rate it creates lots of air pollution in the environment. As the air pollution rate due to burning plastic increases then there is a dramatic rise in air pollution. From

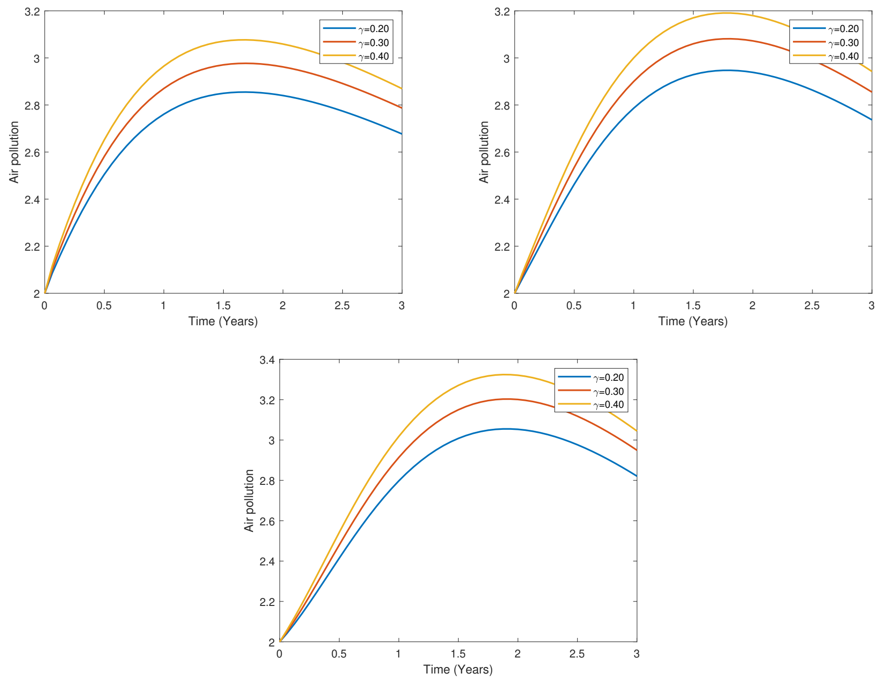

Figure 7. Effect of air pollution due to recycling plastic on air pollution for (a) $\alpha = 0.8$ (b) $\alpha = 0.9$ (c) $\alpha = 1$.

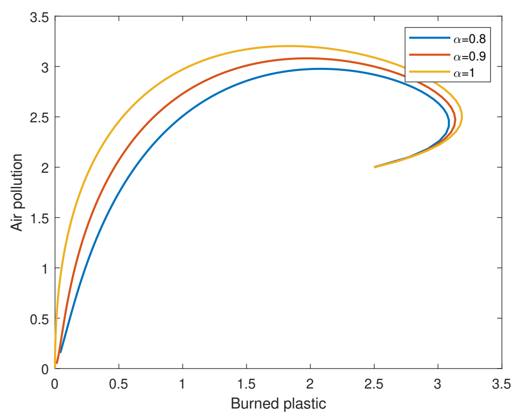

Figure 8. Phase diagram of burned plastic against air pollution.

Figure 7, it is observed that as the plastic is recycled at high temperatures also it creates lots of air pollution. As the air pollution rate due to recycled plastic increases then there is a dramatic rise in air pollution.

Figure 8 shows the phase diagram of burned plastic against air pollution whereas Figure 9 shows the phase diagram of recycled plastic against air pollution. Both the results reveal that as the burning rate or recycling rate of plastic increases then air pollution increases whereas the burning rate or recycling rate of plastic decreases then air pollution decreases. Also, the graphical results reveal that as the burning and recycling process is terminated temporarily then the air pollution

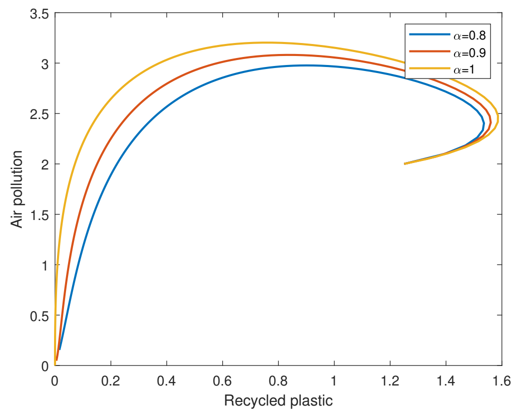

Figure 9. Phase diagram of recycled plastic against air pollution.

through burning and recycling of plastic also tends to zero. Thus there is a strong positive correlation between the burning rate and air pollution through plastic and the recycled rate and air pollution through plastic.

6. Conclusion

In this paper, we presented a mathematical model for plastic waste for the transmission dynamics of burned plastic and recycled plastic on air pollution. The qualitative, and quantitative behavior and reproduction number were computed. The analysis shows that the model possesses three equilibrium points namely the pollution-free, recycling-free, and endemic equilibrium points. The PFE point, RFE point, and EEP point are locally asymptotically stable if $R_0 < 1$ and under the condition (4.19), (4.25), and (4.30) respectively. The EEP point is globally asymptotically stable if $R_0 > 1$, otherwise unstable. The numerical results show that the process of burning plastic and recycling plastic is an important strategy to reduce waste plastic. Furthermore, air pollution is only reduced if plastic production is reduced and promote the reuse of plastic. Burning plastic and recycling plastic restrict plastic waste. Still, for the optimal solution of plastic waste and air pollution, we altogether make an effort to cut down the usage of plastic and promote the reuse of plastic. In the future, the present model can be extended to study the effects of plastic waste on air pollution along with cardiovascular diseases and nervous system.

Acknowledgements

No funding to declare. The authors thank the editor and reviewers for their comments and suggestions to improve the paper considerably.

Competing interests. The authors have no competing interests to declare.

Data availability statement. No Data associated in the manuscript.

References

[1] Y. N. Anjam, M. Yavuz, M. ur Rahman and A. Batool, *Analysis of a fractional pollution model in a system of three interconnecting lakes*, AIMS Biophys., 2023, 10(2), 220–240.

[2] D. Baleanu, S. M. Aydogan, H. Mohammadi and S. Rezapour, *On modelling of epidemic childhood diseases with the Caputo-Fabrizio derivative by using the Laplace Adomian decomposition method*, Alexandria Eng. J., 2020, 59(5), 3029–3039.

[3] D. Baleanu, K. Diethelm, E. Scalas and J. J. Trujillo, *Fractional Calculus: Models and Numerical Methods*, World Sci., 2012.

[4] M. Barma, H. K. Biniyamin, U. M. Modibbo and H. M. Gaya, *Mathematical model for the optimization of municipal solid waste management*, Front. Sustain., 2022, 3, 18.

[5] A. Chatterjee and S. Pal, *A predator-prey model for the optimal control of fish harvesting through the imposition of a tax*, Int. J. Optim. Control: Theor., 2023, 13(1), 68–80.

[6] S. Chaturvedi, B. P. Yadav, N. A. Siddiqui and S. K. Chaturvedi, *Mathematical modelling and analysis of plastic waste pollution and its impact on the ocean surface*, J. Ocean Eng. Sci., 2020, 5(2), 136–163.

[7] J. Chu, H. Liu and A. Salvo, *Air pollution as a determinant of food delivery and related plastic waste*, Nat. Hum. Behav., 2021, 5(2), 212–220.

[8] J. Colwell, S. Pratt, P. Lant and B. Laycock, *Hazardous state lifetimes of biodegradable plastics in natural environments*, Sci. Total Environ., 2023, 165025.

[9] J. Danane, M. Yavuz and M. Yıldız, *Stochastic modeling of three-species Prey–Predator model driven by Lévy jump with mixed holling-II and Beddington–DeAngelis functional responses*, Fractal Fract., 2023, 7(10), 751.

[10] F. Degli-Innocenti, M. Barbale, S. Chinaglia, E. Esposito, M. Pecchiari, F. Razza and M. Tosin, *Analysis of the microplastic emission potential of a starch-based biodegradable plastic material*, Polym. Degrad. Stab., 2022, 199, 109934.

[11] O. Diekmann, J. A. P. Heesterbeek and M. G. Roberts, *The construction of next-generation matrices for compartmental epidemic models*, J. R. Soc. Interface, 2010, 7(47), 873–885.

[12] K. Diethelm, *The Analysis of Fractional Differential Equations: An Application-Oriented Exposition Using Differential Operators of Caputo Type*, Springer-Verlag Berlin Heidelberg, 2010.

[13] K. Diethelm, N. J. Ford and A. D. Freed, *A predictor-corrector approach for the numerical solution of fractional differential equations*, Nonlinear Dyn., 2002, 29, 3–22.

[14] F. Evirgen, F. Ozköse, M. Yavuz and N. Ozdemir, *Real data-based optimal control strategies for assessing the impact of the Omicron variant on heart attacks*, AIMS Bioeng., 2023, 10, 218–239.

[15] F. Evirgen, E. Uçar, S. Uçar and N. Özdemir, *Modelling influenza a disease dynamics under Caputo-Fabrizio fractional derivative with distinct contact rates*, Mathematical Modelling and Numerical Simulation with Applications, 2023, 3(1), 58–72.

[16] F. Evirgen and M. Yavuz, *An alternative approach for nonlinear optimization problem with Caputo-Fabrizio derivative*, in ITM Web of Conferences, EDP Sciences, 2018, 22, 01009.

[17] B. Fatima, M. Yavuz, M. ur Rahman, A. Althobaiti and S. Althobaiti, *Predictive modeling and control strategies for the transmission of middle east respiratory syndrome coronavirus*, Mathematical and Computational Applications, 2023, 28(5), 98.

[18] T. P. Haider, C. Völker, J. Kramm, K. Landfester and F. R. Wurm, *Plastics of the future? The impact of biodegradable polymers on the environment and on society*, Angewandte Chemie International Edition, 2019, 58(1), 50–62.

[19] M. Izadi, M. Parsamanesh and W. Adel, *Numerical and stability investigations of the waste plastic management model in the ocean system*, Math., 2022, 10(23), 4601.

[20] A. Jha, N. Adlakha and B. K. Jha, *Finite element model to study effect of Na+ - Ca2+ exchangers and source geometry on calcium dynamics in a neuron cell*, J. Mech. Med. Biol., 2015, 16(2), 1–22.

[21] B. K. Jha and H. Joshi, *A fractional mathematical model to study the effect of buffer and endoplasmic reticulum on cytosolic calcium concentration in nerve cells*, in Fractional Calculus in Medical and Health Science, Boca Raton, FL: CRC Press/Taylor & Francis Group, [2021]: CRC Press, 2020, 211–227.

[22] B. K. Jha, V. H. Vatsal and H. Joshi, *A fractional approach to study of calcium advection distribution and VGCC in astrocyte*, in 2023 International Conference on Fractional Differentiation and its Applications, 2023, (ICFDA), IEEE, 1–5. DOI: 10.1109/ICFDA58234.2023.10153226.

[23] H. Joshi and B. K. Jha, *A mathematical model to study the role of buffer and ER flux on calcium distribution in nerve cells*, in Mathematical Modeling, Computational Intelligence Techniques and Renewable Energy: Proceedings of the First International Conference, MMCITRE 2020, 2021, 1287, 265–273.

[24] H. Joshi and B. K. Jha, *2D memory-based mathematical analysis for the combined impact of calcium influx and efflux on nerve cells*, Comput. Math. Appl., 2023, 134, 33–44.

[25] H. Joshi and M. Yavuz, *Transition dynamics between a novel coinfection model of fractional-order for COVID-19 and tuberculosis via a treatment mechanism*, Eur. Phys. J. Plus, 2023, 138(5), 468.

[26] H. Joshi, M. Yavuz and I. Stamova, *Analysis of the disturbance effect in intracellular calcium dynamic on fibroblast cells with an exponential kernel law*, Bulletin of Biomathematics, 2023, 1(1), 24–39.

[27] H. Joshi, M. Yavuz, S. Townley and B. K. Jha, *Stability analysis of a non-singular fractional-order COVID-19 model with nonlinear incidence and treatment rate*, Phys. Scr., 2023, 98(4), 045216.

[28] Q. V. Khuc, T. Dang, M. Tran, D. T. Nguyen, T. Nguyen, P. Pham and T. Tran, *Household-level strategies to tackle plastic waste pollution in a transitional country*, Urban Science, 2023, 7(1), 20.

[29] P. Kumar and V. S. Erturk, *Dynamics of cholera disease by using two recent fractional numerical methods*, Mathematical Modelling and Numerical Simulation with Applications, 2021, 1(2), 102–111.

[30] M. Y. Li, H. L. Smith and L. Wang, *Global dynamics of an seir epidemic model with vertical transmission*, SIAM J. Appl. Math., 2001, 62(1), 58–69.

[31] R. L. Magin, *Fractional Calculus in Bioengineering*, Begell House, 2006.

[32] D. Matignon, *Stability results for fractional differential equations with applications to control processing*, Comput. Eng. Syst. Appl., 1996, 2(1), 963–968.

[33] A. Munson, *A harmonic oscillator model of atmospheric dynamics using the Newton-Kepler planetary approach*, Mathematical Modelling and Numerical Simulation with Applications, 2023, 3(3), 216–233.

[34] P. A. Naik, Z. Eskandari, H. E. Shahkari and K. M. Owolabi, *Bifurcation analysis of a discrete-time prey-predator model*, Bulletin of Biomathematics, 2023, 1(2), 111–123.

[35] P. A. Naik, M. Yavuz, S. Qureshi, J. Zu and S. Townley, *Modeling and analysis of COVID-19 epidemics with treatment in fractional derivatives using real data from Pakistan*, Eur. Phys. J. Plus, 2020, 135(10), 1–42.

[36] P. A. Naik, M. Yavuz and J. Zu, *The role of prostitution on HIV transmission with memory: A modeling approach*, Alexandria Eng. J., 2020, 59(4), 2513–2531.

[37] I. Podlubny, *Fractional Differential Equations: An Introduction to Fractional Derivatives, Fractional Differential Equations, to Methods of their Solution and some of their*, 1st Editio. Academic Press, Elsevier, 1998.

[38] D. G. Prakasha, P. Veeresha and H. M. Baskonus, *Analysis of the dynamics of hepatitis E virus using the Atangana-Baleanu fractional derivative*, Eur. Phys. J. Plus, 2019, 134(5), 1–11.

[39] P. Rana, K. Chaudhary, S. Chauhan, M. Barik and B. K. Jha, *Dynamic analysis of mother-to-child transmission of hiv and antiretroviral treatment as optimal control*, Commun. Math. Biol. Neurosci., 2022, 2022, 45.

[40] S. G. Samko, A. A. Kilbas and O. I. Marichev, *Fractional Integrals and Derivatives: Theory and Applications*, Gordon and Breach Science Publishers, 1993.

[41] N. A. Shah, A. O. Popoola, T. Oreyeni, E. Omokhuale and M. M. Altine, *A modelling of bioconvective flow existing with tiny particles and quartic autocatalysis reaction across stratified upper horizontal surface of a paraboloid of revolution*, Mathematical Modelling and Numerical Simulation with Applications, 2023, 3(1), 74–100.

[42] T. Singh, Vaishali and N. Adlakha, *Numerical investigations and simulation of calcium distribution in the alpha-cell*, Bulletin of Biomathematics, 2023, 1(1), 40–57.

[43] M. F. Tabassum, et al., *Differential gradient evolution plus algorithm for constraint optimization problems: A hybrid approach*, Int. J. Optim. Control: Theor., 2021, 11(2), 158–177.

[44] A. B. Tufail, et al., *Deep learning in cancer diagnosis and prognosis prediction: A minireview on challenges, recent trends, and future directions*, Comput. Math. Methods Med., 2021, 2021, 1–28.

[45] C. Vargas-De-León, *Volterra-type Lyapunov functions for fractional-order epidemic systems*, Commun. Nonlinear Sci. Numer. Simul., 2015, 24(1–3), 75–85.

[46] G. C. Vega, A. Gross and M. Birkved, *The impacts of plastic products on air pollution-A simulation study for advanced life cycle inventories of plastics covering secondary microplastic production*, Sustain. Prod. Consum., 2021, 28, 848–865.

[47] World Health Organization, *Ambient (Outdoor) Air Pollution* [Online]. Available: https://www.who.int/news-room/fact-sheets/detail/ambient-(outdoor)-air-quality-and-health?$gclid = Cj0KCQjwjryjBhD0ARIsAMLvnF_BTgKJn9hxKSPP5mxQIKqoMhuVQKGe1KRKDSYpR5 - vOxcJtKXFgLgaAqEoEALw_wcB$. [Accessed: 25-May-2023].

[48] S. Zhang, et al., *Microplastics in the environment: A review of analytical methods, distribution, and biological effects*, Trends Analyt Chem., 2019, 111, 62–72.